

AD-A244 253



**S** **D**  
JAN 07 1992

Vertical Velocity Generated  
over

Non-homogeneous Rough Terrain,  
Theory and Subgrid-Scale Parameterization

G.A. Dalu<sup>1,3</sup>, T.J. Lee<sup>2</sup>, M. Segal<sup>2</sup>, R.A. Pielke<sup>2</sup>, and A. Guerrini<sup>3</sup>

February 2, 1990

- 1 - mailing address: G.A. Dalu, Cooperative Institute for Research in the Atmosphere, CIRA-CSU, Foothill Campus, Fort Collins, Colorado 80523
- 2 - Department of Atmospheric Science, Colorado State University, CSU, Fort Collins, Colorado
- 3 - Institute for Atmospheric Physics, IFA-CNR, Rome

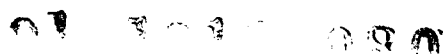
**Abstract**

A systematic evaluation of vertical velocities associated with stratified atmospheric flows over non-homogeneous terrains apparently has not been reported in the literature. In this study we approach the problem numerically and analytically. Through a non-linear model we evaluate the range of the parameters for validity of the linear theory. Through simple analytical theory we estimate the role played by the relevant parameters.

Results indicate that, when the transition in surface roughness is gradual between a smooth and a rough surface, the perturbation of the vertical velocity has the same horizontal scale as the perturbing source. The nature of the perturbation depends on the product between the horizontal scale of the rough patch and the Scorer parameter of the ambient atmosphere; i.e. very small values of this product (weakly stratified atmosphere) gives a wave trapped around the top of the stress layer, while values of the order of unity give a non-hydrostatic gravity wave which propagates away from the top of the stress layer. Values larger than unity yield a propagating hydrostatic wave.

This document has been approved for public release and sale; its distribution is unlimited.

91-18128



• When the transition in surface roughness is abrupt, the wave is nonhydrostatic with a horizontal and vertical wave number equal to the ambient Scorer parameter. When the product between the horizontal width of the rough patch and the Scorer parameter is large, there is no significant interference between the wave upstream and the wave downstream of the rough patch; the two waves are of the same nature and amplitude, but opposite sign. When this product is small, however, the wave upstream interferes destructively with the wave downstream, i.e. the amplitude of the resulting wave is accordingly reduced.

When the surface roughness is periodic, resonant amplification occurs when the horizontal wave number of the perturbation approaches the ambient Scorer parameter.

Since the depth of updraft well exceeds the height of the internal boundary layer, this process can be important in triggering cumulus clouds and may have an impact on the dispersion of pollutants.

## 1 Introduction

When an air mass approaches a region where there is a substantial increase in surface roughness, we expect a decrease of the air speed in the lower layer and the development of ascent associated with the resultant horizontal convergence. Such situations are typical, for example, in coastal urban areas when onshore flow occurs. However, it may also be of significance in inland urban areas, because of the contrast with surrounding agricultural rural areas or when there is a contrast between prairie and wooded areas. The developed vertical velocities may trigger, under supportive synoptic conditions, convective clouds. The features of the induced vertical velocity may also have an importance in dispersing pollutants.

In this paper we approach the problem of the vertical velocity which arises because of horizontal inhomogeneities in the surface shearing stress in the atmospheric planetary boundary layer. This study is an extension in more general terms of a previous paper (Dalu *et al.* 1988), where we report on the waves generated by change in surface roughness.

Numerous studies have been carried out evaluating the impact of a sudden change in the surface roughness on horizontal flow features in a neutrally stratified boundary layer, focusing mainly on the modification of the flow within the surface layer. In addition, considerable attention has been given to evaluate the growth of thermal and aerodynamics internal boundary layers. Hunt and

Simpson (1982) provide an excellent review of the studies reported by that time. Additional studies reporting on the impact of a sudden change in the surface roughness on the horizontal flow are given by Pedergrass and Arya (1984).

Overall, however, no systematic attention has been given in the evaluation of the features of the vertical velocities generated in a stable stratified flow when the air crosses a change in the surface roughness (CSR). Wagner (1966) reported on the structure of the vertical velocity induced by a CSR as computed through a numerical model. However, he neglected to discuss the vertical extensions of the updraft and its wave characteristics, because of his upper boundary condition: in fact he required the vertical velocity to be zero and the flow to be in geostrophic balance at 1000 meters above the ground.

Claussen (1986) computed, using a model simulation, the vertical velocity due to a CSR. However, the computed vertical velocity was, in general, very sensitive to the horizontal grid resolution, which should be reduced, in many occasions, to several hundred meters in order to appropriately resolve the related vertical velocity.

Using a very coarse horizontal resolution, Vukovich and Dunn (1978) in their numerical model simulation of the St. Louis urban area, suggested that the surface roughness has only a small effect on the circulation for the wind speeds used in their study. Alestalo *et al.* (1985), using a hydrostatic two-dimensional model with a grid interval of 4 km simulated the airflow in the Baltic shore region of Finland, and found a maximum for the vertical velocity of order of  $1 \text{ cm s}^{-1}$ , due to the CSR. They attributed the reported increase of precipitation in that area, in the absence of thermal forcing, to the vertical velocity induced by the CSR. Pielke (1974) evaluated the magnitude of vertical velocity caused by a CSR over Florida using a 11 km horizontal resolution model. Although the magnitudes were small ( $\approx 0.1 \text{ cm s}^{-1}$ ), it was concluded that shallow warm rain cloud over the southeast coast of Florida could be due to this mechanism. Finally, Roeloffzen *et al.* (1986) presented a steady state model calculation of secondary flow patterns forced by a CSR. Adopting a neutral boundary layer and using a refined grid resolution, they suggest that frictional effects involved with a CSR at a coast line, can lead to a secondary circulation on the mesoscale. They suggest that this forcing is a factor in the observed coastal frontogenesis active in the early fall along the coast of the Netherlands.

Statement A per telecon  
Dr. Robert Abbey ONR/Code 1122  
Arlington, VA 22217-5000  
NWW 1/6/92

SEARCHED BY _____	
Date	Author/Editor/Speller
A-1	

The present study presents a systematic analytical and numerical evaluation of *CSR* impact in a stably stratified air mass, for an one-layered atmosphere and in a two-layered atmosphere, on the generation of vertical velocities and their characteristics as dependent on key parameters including the wind speed, the thermal stratification of the lower atmosphere, and the magnitude of the shearing stress.

The results of this study are confirmed by the general mesoscale features observed during the Amazon Boundary Layer Experiment *ABLE 2B* (Garstang *et al*, 1990). However, the present theory should be extended to include the diabatic sources, in order to explain the *ABLE 2B* results in a more quantitative way.

## 2 Waves Generated by a *CSR* as Simulated by a Numerical Model

Here we present some results concerning the vertical velocity induced by a sudden change in terrain surface roughness, as simulated by a numerical model. For the simulation we use the non-hydrostatic version on an  $f$ -plane of the CSU Regional Atmospheric Meteorological Model *RAMS* (Tremback *et al*, 19...??). The ambient flow is perpendicular to the *CSR*, and the atmosphere is stable stratified. We assume a sudden change of roughness  $z_o = 1$  m, and a flow intensity of  $U = 5$  m s<sup>-1</sup> and  $U = 10$  m s<sup>-1</sup>. We show the results after a few hours of simulation, i.e. when the system evolves to an almost steady state. Results for an ambient flow of  $U = 5$  m s<sup>-1</sup> are shown in Fig.1 and for an ambient flow of  $U = 10$  m s<sup>-1</sup> in Fig.2. The results in Fig.1 and in Fig.2 show that substantial vertical velocities can be induced by a sudden change of surface roughness and that the perturbation is of a wave nature (since the atmosphere is stratified) with a wave length and intensity which doubles for a doubling of the wind intensity. This response suggests a linear behavior.

The non-linear behavior is apparently confined to within the stress layer, which in the numerical model is parameterized according a turbulent kinetic energy *TKE* scheme (Deardorf, 1980). As a consequence, the depth of the stress layer and the shear velocity do not respond linearly to the variations of the flow intensity.

However, from the simulations completed with the nonlinear model, we found that for  $\Delta U/U < .2$  with the largest perturbation near the surface, i.e. the relative perturbation of the horizontal

velocity is less than 20% (similar results have been found by Claussen, 1987). Thus we deduce that the response in the atmosphere above the stress layer is linear and that the non-linearities are confined to the turbulence within the stress layer.

We proceed in investigating the nature of the perturbation through linear analytical theory, in order to find simple relations between the behavior shown in Fig.1 and in Fig.2 and the ambient parameters. In the following theoretical study, we assume the depth and the intensity of the stress, which can be obtained through observations or turbulence theory.

### 3 The Governing Equation for the Linear Problem

If we assume that the process is stationary, two-dimensional and Boussinesq, then the primitive equations in linear form can be reduced to a Scorer type equation for the vertical velocity in non-homogeneous form:

$$\left( \frac{k^2 - k_o^2}{k^2} \right) \hat{w}_{zz} + (l^2 - k^2) \hat{w} = \frac{\hat{\tau}_{zz}}{\rho U} = \frac{u_*^2}{U} \quad (3.1)$$

The linearization is justified by fact that the non-linear numerical simulations have shown that the perturbations are small in comparison to the intensity of the ambient wind, see section (2). For a derivation of equation (3.1), see Eliassen (1977). The hat denotes the Fourier transform of the variable,  $k$  is the horizontal wave number,  $k_o = f/U$  is the inertial wave number, ( $f$  is the Coriolis parameter,  $U$  is the ambient flow perpendicular to the change in surface roughness, and  $U_z$  is its shear),  $\tau$  is the resulting shear stress,  $u_*$  is the shear velocity, and  $l$  is the Scorer parameter (Scorer, 1953):

$$l^2 = \frac{N^2}{U^2} - \frac{U_{zz}}{U} \quad \text{with} \quad N^2 = \frac{\partial \bar{b}}{\partial z} \quad (3.2)$$

where  $N$  is the Brunt-Väisälä frequency and  $\bar{b}$  is the buoyancy of the environment. Equation (3.1) can be rewritten as:

$$\hat{w}_{zz} + \nu^2(k) \hat{w} = G^2(k) \frac{\hat{\tau}_{zz}}{\rho U} = G^2(k) \frac{u_*^2}{U} \quad (3.3)$$

$$\text{with} \quad \nu^2(k) = k^2 \frac{l^2 - k^2}{k^2 - k_o^2} \quad \text{and} \quad G^2(k) = \frac{k^2}{k^2 - k_o^2}$$

In the wave number region where  $\nu^2(k) < 0$ , the waves are trapped around the perturbing source within an  $\epsilon$ -folding vertical distance equal to  $\mu_0^{-1}$ . The vertical wave number  $\mu_0$  for the trapped waves is:

$$\mu_0(k) = |i \nu(k)| = |k| \sqrt{\frac{l^2 - k^2}{k_o^2 - k^2}} \quad \text{when } 0 < |k| < k_o \quad \text{or when } l < |k| < \infty \quad (3.4)$$

In the wave number region where  $\nu^2(k) > 0$ , the waves propagate away from the perturbing source with a vertical wave number equal to  $\mu_1$ . The vertical wave number  $\mu_1$  for the propagating waves is:

$$\mu_1(k) = \nu(k) = k \sqrt{\frac{l^2 - k^2}{k^2 - k_o^2}} \quad \text{when } k_o < |k| < l. \quad (3.5)$$

### 3.1 The Stress and the Shear Velocity

For simplicity, we assume that the stress has the same direction and opposes the ambient flow. Furthermore, since the stress is assumed to decay linearly with altitude within the stress layer (this simple choice is suggested by the results of the numerical simulations; i.e. see section (2)):

$$\tau(x, z) = \tau_o H\epsilon(h - z) \frac{h - z}{h} F(x) \quad (3.6)$$

where  $\tau_o$  is the surface shear stress,  $F(x)$  is its horizontal distribution, and  $H\epsilon$  is the Heaviside function. We study the atmospheric response

to a periodic horizontal distribution of the stress:

$$\text{case (i)} \quad \tau_{zz}(x, z) = \frac{\tau_o \delta(z - h)}{h^2} \cos(\alpha x) \Rightarrow \tilde{\tau}_{zz}(k, z) = \frac{\tau_o \delta(z - h) \pi}{h^2} \delta(k - \alpha) \quad (3.7)$$

to a bell shape horizontal distribution of the stress:

$$\text{case (ii)} \quad \tau_{zz}(x, z) = \frac{\tau_o \delta(z - h)}{h^2} \frac{a^2}{a^2 + x^2} \Rightarrow \tilde{\tau}_{zz}(k, z) = \frac{\tau_o \delta(z - h) \pi a}{h^2} \exp(-ak); \quad (3.8)$$

and to a top hat horizontal distribution of the stress:

$$\text{case (iii)} \quad \tau_{zz}(x, z) = \frac{\tau_o \delta(z - h)}{h^2} [H\epsilon(x + a) - H\epsilon(x - a)] \Rightarrow \tilde{\tau}_{zz}(k, z) = \frac{\tau_o \delta(z - h) \sin(ka)}{h^2 k} \quad (3.9)$$

Here  $\delta$  is the Dirac function. The tilde denotes the cosine Fourier transform:

$$\tilde{F}(k) = \int_0^\infty dx F(x) \cos(kx)$$

The relation between the stress  $\tau$ , the wind intensity  $U$ , the surface drag  $C_D$ , and the shear velocity  $u^*$  is given by (Panofsky and Dutton, 1984):

$$\frac{u^{*2}}{U} = \frac{\tau_o}{\rho U} = C_D U \quad \text{with} \quad C_D = \left(\frac{u^*}{U}\right)^2 = O\left(\frac{\kappa^2}{(\ln z/z_o)^2}\right) \quad (3.10)$$

Here  $\kappa$  is the von Karmann constant and  $z_o$  is the surface roughness. The order of magnitude of the depth of the stress layer is (Blackadar and Tenneks, 1968):

$$h \approx 0.3 \frac{u^*}{f} \quad \text{so that} \quad lh \approx 0.3 \frac{lu^*}{f} = 0.3 C_D \frac{N}{f} \quad (3.11)$$

These simple formulas give a shear velocity and a stress layer which grow almost linearly with the wind intensity, with a depth almost a constant fraction of the inverse of the Scorer parameter.

However, results from the non-linear model (section 2) show that the the shear velocity and the stress layer grow almost linearly with the wind intensity when the wind is weak; their growth is slower than linear at a higher wind speed. The quantification of this result is rather sensitive to the turbulence scheme used.

#### 4 Atmospheric Response to a Roughness Changes

The atmospheric response to a general surface roughness change is given by:

$$w(x, z) = I_{o_1} + I_1 + I_{o_2} = \frac{2\bar{w}}{\pi} \left\{ \int_0^{k_o} dk G_o(k) w_{\mu_o}(k, z) \bar{F}(k) + \int_{k_o}^l dk G_1(k) w_{\mu_1}(k, z) \bar{F}(k) + \int_l^\infty dk G_o(k) w_{\mu_o}(k, z) \bar{F}(k) \right\} \quad \text{with} \quad \bar{w} = \frac{\tau_o}{\rho U} \frac{1}{lh} = \frac{u^{*2}}{U} \frac{1}{lh} \quad (4.1)$$

Where  $\bar{w}$  is the amplitude of the perturbation of the vertical velocity. Here

$$G_o(k) = -\frac{lG^2(k)}{\mu_o(k)} = \frac{lk}{\sqrt{(k_o^2 - k^2)(l^2 - k^2)}} \quad \text{and} \quad G_1(k) = \frac{lG^2(k)}{\mu_1(k)} = \frac{lk}{\sqrt{(k^2 - k_o^2)(l^2 - k^2)}} \quad (4.2)$$

The  $w_{\mu_o}(k, z)$  waves are trapped around the top of the stress layer:

$$w_o(k, z) = \{He(z - h) \exp(-\mu_o(z - h)) + [He(z) - He(z - h)] \exp(-\mu_o(h - z))\}$$

$$-He(z) \exp(-\mu_o(z+h))\} \cos(kx) \quad (4.3)$$

In eq. (4.3) the first and the second term give waves which are trapped over and below the top of the stress layer, respectively. Since these waves have their maximum amplitude at the top of the stress layer, they may have a role in triggering cumulus convection, even if their amplitude decays exponentially with distance; the third term is the wave reflected from the ground, (see Appendix).

The  $w_{\mu_1}(k, z)$  waves propagate away from the top of the stress layer:

$$w_{\mu_1}(k, z) = \{He(z-h) \sin(\mu_1(z-h) + kx) + [He(z) - He(z-h)] \sin(\mu_1(h-z) + kx) - He(z) \sin(\mu_1(z+h) + kx)\} \quad (4.4)$$

In eq. (4.4) the first term is the wave which propagates upward, the second term is the wave which propagates downward, and the third term is the wave reflected from the ground, (see Appendix).

We assume the following values for environment parameters (when the atmosphere is stratified):  $N = 10^{-2} \text{ sec}^{-1}$ ,  $U = 10 \text{ m s}^{-1}$ ,  $u^* = 20 \text{ cm s}^{-1}$ , and  $f = 10^{-4} \text{ s}^{-1}$ , then we have  $l = 10^{-3} \text{ m}^{-1}$ ,  $k_o = 10^{-5} \text{ m}^{-1}$ ,  $h = 300 \text{ m}$ ; and  $N = l = 0.0$  when the environment is non-stratified.

#### 4.1 Resonant amplification due to periodicity, (case (i))

When the surface roughness is periodic (eq. (3.7)) the vertical velocity is given by:

$$w(x, z) = \bar{w} \{G_o(\alpha)w_{\mu_o}(\alpha, z) + G_1(\alpha)w_{\mu_1}(\alpha, z)\} \quad (4.5)$$

$$\text{Where } G_o(\alpha) = \frac{l\alpha}{\sqrt{(k_o^2 - \alpha^2)(l^2 - \alpha^2)}} \quad \text{and} \quad G_1(\alpha) = \frac{l\alpha}{\sqrt{(\alpha^2 - k_o^2)(l^2 - \alpha^2)}} \quad (4.6)$$

$$\text{with } w_o(\alpha, z) = - \{He(z-h) \exp(-\mu_o(z-h)) + [He(z) - He(z-h)] \exp(-\mu_o(h-z)) - He(z) \exp(-\mu_o(z+h))\} \cos(\alpha x) \quad (4.7)$$

$$\text{and with } w_{\mu_1}(\alpha, z) = \{He(z-h) \sin(\mu_1(z-h) + \alpha x) + [He(z) - He(z-h)] \sin(\mu_1(h-z) + \alpha x) - He(z) \sin(\mu_1(z+h) + \alpha x)\} \quad (4.8)$$



$$\mu_o = \alpha \sqrt{\frac{l^2 - \alpha^2}{k_o^2 - \alpha^2}} \quad \text{and} \quad \mu_1 = \alpha \sqrt{\frac{l^2 - \alpha^2}{\alpha^2 - k_o^2}}$$

The amplitude  $G_o(\alpha)$  of the trapped wave and the amplitude  $G_1(\alpha)$  of the propagating wave are amplified by resonance when  $\alpha = l$ , i.e.  $G_o(\alpha \rightarrow l) \rightarrow \infty$  and  $G_1(\alpha \rightarrow l) \rightarrow \infty$ . When the wave number  $\alpha$  of the rough patch distribution approaches the ambient Scorer parameter  $l$ , the maximum enhancement of the vertical velocity occurs.

There is a resonance also at  $\alpha = k_o$ , but this resonance is canceled by infinitely rapid oscillations  $\mu_1(\alpha \rightarrow l) \rightarrow \infty$ , or by infinitely strong trapping,  $\mu_o(\alpha \rightarrow l) \rightarrow \infty$ .

## 4.2 Vertical velocity excited by a bell shaped stress, (case (ii))

In this section we study the vertical velocity induced by a rough patch, in relation to its horizontal extension. The bell shape distribution is ideal for this kind of analysis, as shown by Queney (1947) and by Smith (1979) for the vertical velocity induced by a bell shape mountain. For a bell-shaped distributed stress case (ii), from eq. (4.1) the vertical velocity is given by:

$$w(x, z) = I_{o_1} + I_1 + I_{o_2} = \bar{u} \left\{ \int_0^{k_o} dk G_o(k) w_{\mu_o}(k, z) a \exp(-ak) + \int_{k_o}^l dk G_1(k) w_{\mu_1}(k, z) a \exp(-ak) + \int_l^\infty dk G_o(k) w_{\mu_o}(k, z) a \exp(-ak) \right\} \quad (4.9)$$

Fig.3a shows the atmospheric response to a bell shape horizontal distribution of the stress with  $a = 8 \text{ km}$ , ( $la = 8$ ). Fig.4a shows the atmospheric response to a bell shape horizontal distribution of the stress with  $a = 1 \text{ km}$ , ( $la = 1$ ). The general features, for standard values of wind velocity and atmospheric stratification, are that the vertical wave number equals the Scorer parameter  $l$ , the horizontal extension of the perturbation is of the order of the width  $a$ , and the propagating wave dominates the trapped wave.

Let us examine in more detail the atmospheric response for different widths  $a$ .

### Some useful approximations

(a) - When  $k_o a \approx 1$  or larger,  $I_{o_1} \gg I_1 + I_{o_2}$ , and the wave is trapped

Due to the exponential decay of the Fourier transform of the bell function for increasing values of the wave number, when the rough patch is very very large (i.e. when the horizontal scale is

comparable to the size of the inertial wave), the contributions of the second and third integrals are negligible in comparison to the contribution of the first integral:

$$\begin{aligned}
 w(x, z) &\approx I_{o_1} = \bar{w} \int_0^\infty dk G_o(k) w_{\mu_o}(k, z) a \exp(-ak) \\
 &= \bar{w} \frac{a}{k_o} \left\{ He(z-h) \frac{(a+z-h)^2 - x^2}{[(a+z-h)^2 + x^2]^2} + [He(z) - He(z-h)] \frac{(a+h-z)^2 - x^2}{[(a+h-z)^2 + x^2]^2} \right. \\
 &\quad \left. - He(z) \frac{(a+z+h)^2 - x^2}{[(a+z+h)^2 + x^2]^2} \right\} \quad \text{with } \mu_o = k \quad \text{and} \quad G_o(k) = \frac{k}{k_o} \quad (4.10)
 \end{aligned}$$

Which is a trapped wave. The vertical velocity monotonically decreases with altitude above the stress layer, and its structure does not depend explicitly on stability parameters (although  $h$  may depend on them), as in the Ekman solution.

(b) - When  $la \gg 1$  (but  $k_o a < 1$ ),  $I_1 \gg I_{o_1} + I_{o_2}$ , and the wave is hydrostatic

The trapped wave contribution is negligible in comparison to the contribution of the propagating hydrostatic wave:

$$\begin{aligned}
 w(x, z) &\approx I_1 = \bar{w} \int_0^\infty dk G_1(k) w_{\mu_1}(k, z) a \exp(-ak) \\
 &= \bar{w} \frac{a}{[a^2 + x^2]} \{ He(z-h) [a \sin(\lambda(z-h)) + x \cos(\lambda(z-h))] + [He(z) - He(z-h)] \\
 &\quad [a \sin(\lambda(h-z)) + x \cos(\lambda(h-z))] - He(z) [a \sin(\lambda(z+h)) + x \cos(\lambda(z+h))] \} \quad (4.11)
 \end{aligned}$$

$$\text{with } \mu_1 = l; \quad G_1(k) = 1 \quad \text{and} \quad \lambda = \sqrt{l^2 - k_o^2}$$

When the atmosphere is stratified and the rough patch is large (with no abrupt roughness transitions), the vertical velocity has a hydrostatic wave structure with a vertical wave number equal to the Scorer parameter (corrected because of inertia) and a horizontal scale comparable with the width of the rough patch. Fig.3b shows the hydrostatic waves for  $la = 8$ , (eq. (4.4)), and how well this form approximates the full solution, (eq. (4.9)), shown in Fig.3a.

(c) - When  $la = O(1)$ ,  $I_{o_1} \ll I_1 + I_{o_2}$ , and the wave is non-hydrostatic

When the atmosphere is stratified, but the rough patch is small, the inertial effect is negligible:

$$w(x, z) \approx I_{o_1} + I_{o_2} = \bar{w} \left\{ \int_0^l dk G_1(k) w_{\mu_1}(k, z) a \exp(-ka) \right. \\ \left. + \int_l^\infty dk G_o(k) w_{\mu_o}(k, z) a \exp(-ka) \right\} \quad (4.12)$$

The propagating wave is non-hydrostatic, with a wave number equal to the Scorer parameter:

$$I_1 = \bar{w} la \exp(-la) \frac{\pi}{2} \{ He(z-h) [\sin(l(z-h)) J_o(l(x-z+h)) + \cos(l(z-h)) H_o(l(x-z+h))] \\ + [He(z) - He(z-h)] [\sin(l(h-z)) J_o(l(x+z-h)) + \cos(l(h-z)) H_o(l(x+z-h))] \\ - He(z) [\sin(l(z+h)) J_o(l(x-z-h)) + \cos(l(z+h)) H_o(l(x-z-h))] \}$$

$$\text{with } \mu_1 = l - k \quad \text{and} \quad G_1(k) = \frac{l}{\sqrt{l^2 - k^2}};$$

The near field contribution of the trapped wave comes from large wave numbers and could be written in terms of the incomplete  $\Gamma$  functions, but a good simple approximation is:

$$I_{o_2} = \bar{w} \exp(-la) \left\{ He(z-h) \frac{a(a+z-h)}{[(a+z-h)^2 + x^2]} + [He(z) - He(z-h)] \frac{a(a+h-z)}{[(a+h-z)^2 + x^2]} \right. \\ \left. - He(z) \frac{a(a+z+h)}{[(a+z+h)^2 + x^2]} \right\} \quad \text{with } \mu_o = k \quad \text{and} \quad G_o(k) = 1$$

The perturbation is confined in space, in a region above the rough patch at an altitude equal to the depth of the stress layer.

Since the far field contribution of the trapped wave comes from wave numbers close to the Scorer parameter, the trapped wave contribution is:

$$I_{o_2} = -\bar{w} la \exp(-la) \frac{\pi}{2} N_o(lx) \{ He(z-h) \exp(-l(z-h)) + [He(z) - He(z-h)] \exp(-l(h-z)) \\ - He(z) \exp(-l(z+h)) \quad \text{with } \mu_o = l \quad \text{and} \quad G_o(k) = \frac{l}{\sqrt{k^2 - l^2}} \}$$

The far field contribution of the trapped wave decays exponentially with the distance from the top of the stress layer, therefore interferes with the propagating wave only at  $z \approx h$ , where the trapped wave cancels the propagating wave upstream and strengthens the propagating wave downstream (the Neumann function is even, while the Struve function is odd, with the same asymptotic absolute value), producing a wake of secondary cells downstream at the level of the top of the stress layer.

$J_o$ ,  $H_o$  and  $N_o$  are the zero order Bessel, Struve and Neumann functions, respectively, with the usual convention that even function of negative argument equals the function of the absolute value of the argument, and that an odd function of negative argument equals the negative of the function of the absolute value of the argument.

Summarising, when the atmosphere is stratified and the rough patch is small, the vertical velocity has a wave structure with a horizontal and a vertical wave number equal to the Scorer parameter, with an exponentially decreasing amplitude for a decreasing width of the rough patch.

Fig.4b shows the non-hydrostatic wave for  $la = 1$  and how well approximates the full solution, (eq. (4.9)), shown in Fig.4a.

(d) - When  $la \ll 1$  (but  $\exp(-k_o a) \approx 1$ ),  $I_{o2} \gg I_{o1} + I_1$ , and the flow is irrotational

When the stratification is weak,  $l$  is small, and the contribution of the first and the second integrals in eq. (4.9) can be neglected, only the third integral contributes. Through the use of knowledge that the vertical scale of the perturbation equals the depth of stress layer, we simply have:

$$u(x, z) \approx I_{o2} = \frac{u^*{}^2}{U} \left\{ H\epsilon(z-h) \frac{a(a+z-h)}{[(a+z-h)^2 + x^2]} + [H\epsilon(z) - H\epsilon(z-h)] \frac{a(a+h-z)}{[(a+h-z)^2 + x^2]} - H\epsilon(z) \frac{a(a+z+h)}{[(a+z+h)^2 + x^2]} \right\} \quad \text{with } \mu_o = k \quad \text{and} \quad \bar{w}G_o(k) = \frac{u^*{}^2}{U} \quad (4.13)$$

The vertical velocity monotonically decreases with altitude above the stress layer. Fig.3c shows the trapped waves for  $l = 0.0$  and  $a = 8 \text{ km}$ , (eq. (4.13)). The trapped wave (non-stratified atmosphere) shown in Fig.3c considerably differs from the propagating wave (stratified atmosphere) shown in Fig.3a,b.

### 4.3 Vertical velocity excited by a top hat stress, case (iii)

In this section we study the vertical velocity induced by a rough patch of finite horizontal extension, with very sharp transitions between the smooth and the rough region and *viceversa* ((iii) in eq. 3.9), this is equivalent to problem solved by Lira (1943) for the flow over a step function mountain. From eq. (4.1) the vertical velocity is given by:

$$w(x, z) = \frac{2\bar{w}}{\pi} \left\{ \int_0^{k_0} dk F_0(k) G_0(k) + \int_{k_0}^l dk F_1(k) G_1(k) + \int_l^\infty dk F_0(k) G_0(k) \right\} \quad (4.14)$$

where

$$F_0(k) = \frac{\sin(ka)}{k} w_{\mu_0}(k, z) = \frac{\sin(k(x+a)) - \sin(k(x-a))}{2k} \{ He(z-h) \exp(-\mu_0(z-h)) \\ + [He(z) - He(z-h)] \exp(-\mu_0(h-z)) - He(z) \exp(-\mu_0(z+h)) \} \quad (4.15)$$

$$F_1(k) = \frac{\sin(ka)}{k} w_{\mu_1}(k, z) = \frac{1}{2k} \{ He(z-h) [\cos(\mu_1(z-h) + k(x-a)) - \cos(\mu_1(z-h) + k(x+a))] \\ + [He(z) - He(z-h)] [\cos(\mu_1(h-z) + k(x-a)) - \cos(\mu_1(h-z) + k(x+a))] \\ - He(z) [\cos(\mu_1(z+h) + k(x-a)) - \cos(\mu_1(z+h) + k(x+a))] \} \quad (4.16)$$

From eq. (4.15) and eq. (4.16) we see that the wave at the upstream transition and at the downstream transition are of the same nature, but with an opposite sign. Furthermore, when  $2la = O(1)$ , the wave at the upstream transition (from smooth to rough,  $x = -a$ ) interferes destructively with the wave at the downstream transition (from rough to smooth,  $x = a$ ); and when  $2la \ll 1$  the perturbation becomes negligible, because destructive interference.

The resulting vertical velocity, above the abrupt transition between the smooth and the rough surface (Fig.5a), is given by:

$$w(x, z) = I_{01} + I_1 + I_{02} = \frac{2\bar{w}}{\pi} \left\{ \int_0^{k_0} dk F'_0(k) G_0(k) + \int_{k_0}^l dk F'_1(k) G_1(k) \\ + \int_l^\infty dk F'_0(k) G_0(k) \right\} \quad (4.17)$$

where

$$F'_o(k) = \frac{\sin(k(x+a))}{2k} \{ H\epsilon(z-h) \exp(-\mu_o(z-h)) + [H\epsilon(z) - H\epsilon(z-h)] \exp(-\mu_o(h-z)) - H\epsilon(z) \exp(-\mu_o(z+h)) \} \quad (4.18)$$

$$F'_1(k) = -\frac{1}{2k} \{ H\epsilon(z-h) \cos(\mu_1(z-h) + k(x+a)) + [H\epsilon(z) - H\epsilon(z-h)] \cos(\mu_1(h-z) + k(x+a)) - H\epsilon(z) \cos(\mu_1(z+h) + k(x+a)) \} \quad (4.19)$$

From Fig.6a, we deduce that, when the transition between the smooth and the rough surface is abrupt, the wave is non-hydrostatic with a horizontal and a vertical wave number equal to the Scorer parameter. Since the horizontal scale of the inertial wave is much larger than the inverse of the Scorer parameter, inertia is negligible.

### Some useful approximations

(a) *Wave in a stratified atmosphere,  $I_{o_1} \ll I_1 + I_{o_2}$*

The contribution of the first integral in eq. (4.17) is negligible:

$$w(x, z) \approx I_1 + I_{o_2} = \frac{2\bar{w}}{\pi} \left\{ \int_0^l dk F'_1(k) G_1(k) + \int_l^\infty dk F'_o(k) G_o(k) \right\} = I_1 + I_o \quad (4.20)$$

The propagating wave is non-hydrostatic, with structure similar to a lee mountain wave:

$$I_1 = \frac{\bar{w}}{2} \{ H\epsilon(z-h) [\sin(l(z-h)) H_o(l(x+a-z+h)) - \cos(l(z-h)) J_o(l(x+a-z+h))] + [H\epsilon(z) - H\epsilon(z-h)] [\sin(l(h-z)) H_o(l(x+a+z-h)) - \cos(l(h-z)) J_o(l(x+a+z-h))] - H\epsilon(z) [\sin(l(z+h)) H_o(l(x+a-z-h)) - \cos(l(z+h)) J_o(l(x+a-z-h))] \}$$

$$\mu_1 = l - k \quad \text{and} \quad \frac{G_1(k)}{k} = \frac{1}{\sqrt{l^2 - k^2}};$$

The near field contribution of the trapped wave is:

$$I_{o_2} = \frac{\bar{w}}{\pi} \left\{ H\epsilon(z-h) \tan^{-1} \frac{x+a}{z-h} + [H\epsilon(z) - H\epsilon(z-h)] \tan^{-1} \frac{x+a}{h-z} - H\epsilon(z) \tan^{-1} \frac{x+a}{z+h} \right\}$$

with  $\mu_o = k$  and  $G_o(k) = 1$

The trapped wave contribution is confined above the smooth-rough transition zone, within an  $h$  distance from the top of the stress layer.

In the far field, the trapped wave contribution is:

$$I_{o_2} = \frac{\bar{w}}{2} \text{sign}(x+a) J_o(l(x+a)) \{He(z-h) \exp(-l(z-h)) \\ + [He(z) - He(z-h)] \exp(-l(h-z)) - He(z) \exp(-l(z+h))\}$$

Since the far field contribution comes from wave numbers close to the Scorer parameter, we have assumed:

$$\mu_o = l \quad \text{and} \quad \frac{G_o(k)}{k} = \frac{l}{\sqrt{k^2 - l^2}}$$

The trapped wave, in the far field, decays exponentially with the distance from the top of the stress layer, therefore interferes with the propagating wave only when  $z \approx h$ , where the trapped wave cancels the propagating wave upstream and strengthens the propagating wave downstream, producing a wake of secondary cells downstream at the level of the top of the stress layer.

Fig.5b shows how well (4.20) approximates the upstream transition shown in Fig.5a.

(b) *Trapped wave in a non-stratified atmosphere,  $I_{o_2} \gg I_{o_1} + I_1$*

When the atmosphere is non-stratified, most of the contribution comes from the third intergral in eq. (4.17) and a good approximation of at the abrupt transition between the smooth and the rough surface is:

$$w(x, z) \approx I_{o_2} = \frac{u^{*2}}{\pi U} \left\{ He(z-h) \tan^{-1} \frac{x+a}{z-h} + [He(z) - He(z-h)] \tan^{-1} \frac{x+a}{h-z} \right. \\ \left. - He(z) \tan^{-1} \frac{x+a}{z+h} \right\} \quad \text{with} \quad \mu_o = k \quad \text{and} \quad \bar{w}G_o(k) = \frac{u^{*2}}{U} \quad (4.21)$$

Fig.5c. shows the trapped wave.

#### 4.4 Waves in a two layers atmosphere

The wave emerging from the stress layer is matched with the wave in the free atmosphere using the boundary value Green function defined in the Appendix.

(a) *Wave in the free atmosphere, generated in a non-stratified stress layer*

When the stress layer is non-stratified,  $l' = 0$ , and  $l \neq 0$  in the free atmosphere, the vertical velocity is:

$$w(x, z) \approx \frac{u^{*2}}{\pi U} He(z - h)$$

$$\left\{ h \frac{h[\sin(l(x+a)) - \sin(l(z-h))] - (x+a-z+h)[(1+hl)\cos(l(x+a)) - \cos(l(z-h))]}{(x+a-z+h)^2} \right.$$

$$\left. + h(x+a) \frac{(x+a)^2 + (z-h)^2 - 2h(z-h)}{[(x+a)^2 + (z-h)^2]^2} \right\}$$

$$+ \frac{u^{*2}}{\pi U} \left\{ [He(z) - He(z-h)] \left[ \tan^{-1} \frac{x+a}{h-z} - \tan^{-1} \frac{x+a}{z+h} \right] \right\} \quad (4.22)$$

Fig.6 shows the trasmitted wave.

(b) *Wave ducted within the surface layer*

When the stress layer has a Scorer parameter  $l'$ , with  $l' \gg l \approx 0$ , where  $l$  is the Scorer parameter of the free atmosphere, the wave is ducted between the ground and the top of the stress layer. The vertical velocity is:

$$w(x, z) \approx \frac{\bar{w}}{\pi} \left\{ He(z-h) \tan^{-1} \frac{x+a}{z-h} + [He(z) - He(z-h)] \tan^{-1} \frac{x+a}{h-z} - He(z) \tan^{-1} \frac{x+a}{z+h} \right\}$$

$$+ \frac{\bar{w}}{2} He(z-h) \exp(-l(z-h)) \sum_{m=0}^{\infty} [\sin(2ml'h) H_o(l'(x+a-2mh))$$

$$- \cos(2ml'h) J_o(l'(x+a-2mh)) - \sin(2(m+1)l'h) H_o(l'(x+a-2(m+1)h))$$

$$+ \cos(2(m+1)l'h) J_o(l'(x+a-2(m+1)h))]$$



$$\begin{aligned}
& + \frac{\bar{w}}{2} [He(z) - He(z-h)] \sum_{m=0}^{\infty} [\sin(l'((2m+1)h-z)) H_o(l'(x+a+z-(2m+1)h)) \\
& \quad - \cos(l'((2m+1)h-z)) J_o(l'(x+a+z-(2m+1)h)) \\
& \quad - \cos(l'((2m+1)h-z)) J_o(l'(x+a+z-(2m+1)h)) \\
& \quad + \cos(l'(z+(2m+1)h)) J_o(l'(x+a-z-(2m+1)h))] \tag{4.23}
\end{aligned}$$

The trapped wave contributes only near the smooth-rough transition, because its amplitude decays very rapidly with the number of reflections  $m$ . The wave is fully reflected from the ground, penetrates in the non-stratified free atmosphere a  $l'^{-1}$  distance, and then bounces back towards the ground. Summarising when the stratification in the stress layer is much larger than the one in the above free atmosphere, the wave is ducted between the ground and the top of the stress layer. Fig.7 shows the wave ducted within the stress layer.

## 5 Subgrid-Scale Parameterization

In section 4.1 we have shown that resonant amplification can occur when the distribution of the surface stress is periodic. However it is more realistic to assume that the flow encounters a sudden change of surface roughness, followed by smooth patches alternated with rough patches:

$$\tau_{zz}(x, z) = \frac{\tau_o \delta(z-h)}{h^2} \sum_{n=0}^{\infty} (-1)^n He(x-n a) \tag{5.1}$$

Fig.8 shows the resulting vertical velocity for different value of the product  $la$ , obtained using eq. (4.20). Results shown in Fig.8 contradicts the resonance expected for a periodic surface stress (section 4.1). In fact when  $la = O(1)$  destructive interference starts to take place between the vertical velocity induced by the different patches.

In a subgrid parameterization of the effect of surface roughness in numerical models, we can say that if the rough patches are small in comparison to the inverse of the Scorer parameter, the perturbations interfere destructively and therefore need not be explicitly resolved, but can be averaged beforehand. If the horizontal scale of the rough patches is equal or larger than the inverse of the ambient Scorer parameter, the vertical velocity perturbation needs to be resolved explicitly or parameterized through the use of the theory presented in this paper.

## 6 Conclusions

We have shown that a horizontal change in surface roughness can induce substantial vertical velocity. The vertical velocity can be in the form of a propagating waves, which can penetrate deeply into the atmosphere. The vertical velocity can be in the form of trapped waves as well. In this case the perturbation can be physically relevant, since the maximum is placed at the top of the stress layer, i.e. in the region where it is important to have positive vertical velocities in order to trigger cumulus convection. The nature of this perturbations depends on the enviromental parameter and the horizontal destribution of the surface roughness. In general the vertical wave number is closely related to the ambient Scorer parameter. The horizontal scale of the perturbation equals the scale of the surface roughness when the transition is smooth. For abrupt changes in surface roughness the horizontal scale of the perturbation equals the inverse of the ambient Scorer parameter.

When the horizontal distribution of the rough patches is periodic, resonance amplification can occur when their wave number approaches the value of the ambient Scorer parameter.

**Acknowledgement** This research was made possible by a grant from the National Science Foundation (ATM-8616662) and from the Office of Naval Research (ONR) under contract (N00014-88-K-0029). G.A. Dalu acknowledges the support of CIRA. A. Guerrini and G.A. Dalu acknowledge the support of the Italian project *Clima Territorio e Ambiente nel Mezzogiorno*.

## 7 Appendix

The forced solution of eq. (3.1) is:

$$\begin{aligned}
 w_{forced}(x, z) = & \frac{2}{\pi} \left\{ \int_0^{k_0} dk \int_0^z dz' \frac{\sinh(\mu_0(k)(z-z')) \cos(kx)}{\mu_0(k)} \left( -\frac{G^2(k) \bar{r}_{zz}(k, z')}{\rho U} \right) \right. \\
 & + \int_{k_0}^l dk \int_0^z dz' \frac{\sin(\mu_1(k)(z-z')) \cos(kx)}{\mu_0(k)} \frac{G^2(k) \bar{r}_{zz}(k, z')}{\rho U} \\
 & \left. + \int_l^\infty dk \int_0^z dz' \frac{\sinh(\mu_0(k)(z-z')) \cos(kx)}{\mu_0(k)} \left( -\frac{G^2(k) \bar{r}_{zz}(k, z')}{\rho U} \right) \right\} \quad (7.1)
 \end{aligned}$$

However the first and the third term do not satisfy to the trapped wave condition, and the second term does not satisfy to the radiation condition (Sommerfeld, 1912-48). In order to have meaningful solutions, which satisfy to the physical and to the boundary constraints, we have to add a number of free modes.

Using Green function theory, we seek for the solutions,  $\tilde{g}_o(k, z - z')$  and  $\tilde{g}_1(k, z - z')$ , to the governing equation (3.1) for a point source forcing  $\delta(x', z')$ . If  $\tilde{g}_o(k, z - z')$  and  $\tilde{g}_1(k, z - z')$  satisfy to the boundary condition, and  $\tilde{g}_o(k, z - z')$  satisfies to the trapped wave condition, while  $\tilde{g}_1(k, z - z')$  satisfies to the radiation condition, the total solution for a given forcing is:

$$w_{forced}(x, z) = \left\{ \int_0^{k_o} dk \int_0^z dz' \tilde{g}_o(k, z - z') \left( -\frac{G^2(k) \bar{r}_{zz}(k, z')}{\rho U} \right) + \int_{k_o}^l dk \int_0^z dz' \tilde{g}_1(k, z - z') \frac{G^2(k) \bar{r}_{zz}(k, z')}{\rho U} + \int_l^\infty dk \int_0^z dz' \tilde{g}_o(k, z - z') \left( -\frac{G^2(k) \bar{r}_{zz}(k, z')}{\rho U} \right) \right\} \quad (7.2)$$

### 7.1 Propagating waves and radiation condition

The Green function (the response to a point source  $\delta(x', z')$ ) for the upward propagating wave, which satisfy to the radiation condition, is:

$$\begin{aligned} \tilde{g}_{up}(k, z - z') &= \frac{2}{\pi} H e(z - z') \frac{\sin(\mu_1(k)(z - z')) \cos(kx) + \cos(\mu_1(k)(z - z')) \sin(kx)}{\mu_1(k)} \quad (7.3) \\ &= \frac{2}{\pi} H e(z - z') \frac{\sin(\mu_1(k)(z - z') + kx)}{\mu_1(k)} \end{aligned}$$

The second term in eq. (7.3) is the added free mode.

**Remark** For verification, we derive the boundary value Green function,  $\tilde{g}_{BC}(k, z)$ :

$$\tilde{g}_{BC}(k, z) = - \lim_{z' \rightarrow 0} \left( \frac{\partial}{\partial z'} \tilde{g}_{up}(k, z - z') \right)_{z'=0} = \frac{2}{\pi} \cos(\mu_1(k)z + kx) \quad (7.4)$$

which is the Green function for radiative wave in the mountain problem.

The downward propagating wave is:

$$\tilde{g}_{down}(k, z - z') = \frac{2}{\pi} [H e(z) - H e(z - z')] \frac{\sin(\mu_1(k)(z' - z) + kx)}{\mu_1(k)} \quad (7.5)$$

and the wave reflected from the ground is:

$$\bar{g}_{ref}(k, z - z') = \frac{2}{\pi} H e(z) \frac{\sin(\mu_1(k)(z + z') + kx)}{\mu_1(k)} \quad (7.6)$$

The resulting Green function in the propagating wave region is:

$$\bar{g}_1(k, z - z') = \bar{g}_{up}(k, z - z') + \bar{g}_{down}(k, z - z') - \bar{g}_{ref}(k, z - z') \quad (7.7)$$

## 7.2 Trapped waves

The Green function for the upward trapped wave is:

$$\begin{aligned} \bar{g}_{up}(k, z - z') &= \frac{2}{\pi} H e(z - z') \frac{\sinh(\mu_o(k)(z - z')) - \cosh(\mu_o(k)(z - z'))}{\mu_o(k)} \cos(kx) \\ &= -\frac{2}{\pi} H e(z - z') \frac{\exp(-\mu_o(k)(z - z'))}{\mu_o(k)} \cos(kx) \end{aligned} \quad (7.8)$$

The second term in eq. (7.8) is the added free mode.

**Remark** For verification, we derive the boundary value Green function,  $\bar{g}_{BC}(k, z)$ :

$$\bar{g}_{BC}(k, z) = -\lim_{z' \rightarrow 0} \frac{\partial}{\partial z'} \bar{g}_{up}(k, z - z') = \frac{2}{\pi} \exp(-\mu_o(k)(z - z')) \cos(kx) \quad (7.9)$$

which is the Green function for the trapped wave in the mountain problem.

The downward trapped wave is:

$$\bar{g}_{down}(k, z - z') = -\frac{2}{\pi} [H e(z) - H e(z - z')] \frac{\exp(-\mu_o(k)(z' - z))}{\mu_o(k)} \cos(kx) \quad (7.10)$$

and the wave reflected from the ground is:

$$\bar{g}_{ref}(k, z - z') = -\frac{2}{\pi} H e(z) \frac{\exp(-\mu_o(k)(z + z'))}{\mu_o(k)} \cos(kx) \quad (7.11)$$

The resulting Green function in the trapped wave region is:

$$\bar{g}_o(k, z - z') = \bar{g}_{up}(k, z - z') + \bar{g}_{down}(k, z - z') - \bar{g}_{ref}(k, z - z') \quad (7.12)$$

## References

- Alestalo M. and H. Savijarvi, 1985: Mesoscale circulation in hydrostatic model: coastal convergence and orographic lifting. *Tellus*, **37 A**, 156-162.
- Blackdar, A.K. and H. Tenneks. 1968: Asymptotic similarity in neutral barotropic planetary boundaries. *J. Atm. Sci.* **25** 1015-1020.
- Claussen M., 1987: The flow in a turbulent layer upstream of a change in surface roughness. *Bound. Layer Met.*, **40**, 31-86.
- Tremback *et al* ....., 19.....: Colorado State University Regional Atmospheric Modeling System (CSU-RAMS), on an  $f$ -plane. ....
- Daru G.A., M. Segal, T.J. Lee and R.A. Pielke, 1988: Atmospheric waves induced by change in surface roughness. *Computer Techniques in Environmental Studies*, 551-570. Editor P. Zanetti. Springer-Verlag.
- Deardorf J.W., 1980: Stratocumulus-capped mixed layer derived from a three-dimensional model. *em Bound. Layer Mteo.* **18**, 495-527.
- Eliassen A., 1977: Orographic waves and wave drag: Parameterization of physical effects in the atmosphere. *ECMWF Seminars*, 67-90.
- Garstang M. *et al*, 1990: Amazon Boundary Layer Experiment *ABLE 2B*: A meteorological perspective. *Bull. Am. Met. Soc.*, **71** 19-32.
- Hunt J.C.R. and J.E. Simpson, 1982: Atmospheric boundary layer over non-homogeneous terrain. *Engineering Meteorology*. E.J. Plate Editor Elsevier, 269-318.

- Lyra G., 1943: Theorie der stationären leewellenströmung in freier atmosphäre. *Z. angew. Math. Mech.*, **23** 1-28.
- Panofsky H.A. and J.A. Dutton, 1948: Atmospheric turbulence. John Wiley & Sons. New York, pg 397.
- Pendergrass W. and S.P.S. Arya, 1984: Dispersion in neutral boundary layer over a step change in surface roughness. Mean flow and turbulence structure. *Atm. Env.* **7**, 1267-1279.
- Pielke R.A., 1973: Three-dimensional numerical model of sea breeze over south Florida. Ph.D. thesis, Pen. State Univ.
- Queney P., 1947: Theory of perturbations in stratified currents with application to airflow over mountain barriers. *The University of Chicago Press Mis. Rep.* **23**.
- Roeffzen J.C., W.D. Van Den Berg and J.Oerlemans, 1986: Frictional convergence at coastlines. in *Tellus*, **38 A**, 397-411.
- Smith B.R., 1979: *The influence of mountains on the atmosphere. Advances in Geophysics.* Academic Press. **21** 87-230.
- Sommerfeld A., 1912: Die greensche funktion der schwingungsgleichung. *Jahresber. Dt. Math. Ver.* **21**.
- Sommerfeld A., 1948: Vorlesungen über theoretische physik. Akademische Verlagsgesellschaft. Leipzig **6**. Zweite neubearbeitete Auflage, p.191.

Vukovich F.M. and J.W. Dunn, 1978: A theoretical study of the St. Louis heath island effect: Some parameters variations. *J. Appl. Met.*, **17** 1585-1594.

Wagner M.K., 1966: Two dimensional time dependent numerical model of the atmospheric boundary layer flow over inhomogeneous terrain. Ph.D. thesis, Univ. of Hawaii, 1-80.

## List of Figures

Figure 1. Contours of vertical velocity induced by a sudden change of surface roughness as simulated by a non-linear numerical model.

( $U = 5 \text{ m s}^{-1}$  and  $l = 10^{-3} \text{ m}^{-1}$ )

Figure 2. Contours of vertical velocity induced by a sudden change of surface roughness as simulated by a non-linear numerical model.

( $U = 10 \text{ m s}^{-1}$  and  $l = 10^{-3} \text{ m}^{-1}$ )

Figure 3a. Vertical velocity induced by a bell shaped surface stress in a stratified atmosphere.

( $a = 8 \text{ km}$ ,  $U = 10 \text{ m s}^{-1}$  and  $l = 10^{-3} \text{ m}^{-1}$ )

Figure 3b. Approximate solution.

( $a = 8 \text{ km}$ ,  $U = 10 \text{ m s}^{-1}$  and  $l = 10^{-3} \text{ m}^{-1}$ )

Figure 3c. Approximate solution in a non-stratified atmosphere.

( $a = 8 \text{ km}$ ,  $U = 10 \text{ m s}^{-1}$  and  $l = 0.0 \text{ m}^{-1}$ )

Figure 4a. Vertical velocity induced by a bell shaped surface stress in a stratified atmosphere.

( $a = 1 \text{ km}$ ,  $U = 10 \text{ m s}^{-1}$  and  $l = 10^{-3} \text{ m}^{-1}$ )

Figure 4b. Approximate solution.

( $a = 1 \text{ km}$ ,  $U = 10 \text{ m s}^{-1}$  and  $l = 10^{-3} \text{ m}^{-1}$ )

Figure 5a. Vertical velocity induced by sudden change of surface stress in a stratified atmosphere.

( $U = 10 \text{ m s}^{-1}$  and  $l = 10^{-3} \text{ m}^{-1}$ )

Figure 5b. Approximate solution in a stratified atmosphere.

( $U = 10 \text{ m s}^{-1}$  and  $l = 10^{-3} \text{ m}^{-1}$ )

Figure 5c. Approximate solution in a non-stratified atmosphere.

( $U = 10 \text{ m s}^{-1}$  and  $l = 0.0 \text{ m}^{-1}$ )

Figure 6. Waves in a stratified free atmosphere, generated in a non-stratified stress layer.



$(U = 10 \text{ m s}^{-1}, l = 10^{-3} \text{ m}^{-1} \text{ and } l' = 0.0 \text{ m}^{-1})$

Figure 7. Waves ducted within a stratified stress layer, capped by a weakly stratified free atmosphere.

$(U = 10 \text{ m s}^{-1}, l = 0.0 \text{ m}^{-1} \text{ and } l' = 10^{-3} \text{ m}^{-1})$

Figure 8. Vertical velocity induced by sudden change of surface stress followed by smooth patches alternated with rough patches.

$(a = 0.5, 1, 2, 4, 8 \text{ km}, U = 10 \text{ m s}^{-1} \text{ and } l = 10^{-3} \text{ m}^{-1})$

pg.... and #... refer to the integrals tables by Gradshteyn and Ryzhik

## 8 Derivation of the Approximations

### Bell shape stress

(a) - When  $k_o a \approx 1$  or larger,  $I_{o_1} \gg I_1 + I_{o_2}$ , and the wave is trapped

The contributions of the second and third integrals are negligible in comparison to the contribution of the first integral contribution:

$$\begin{aligned} w(x, z) &\approx \bar{w} \int_0^\infty dk G_o(k) w_{\mu_o}(k, z) a \exp(-ak) \\ &= \bar{w} \frac{a}{k_o} \left\{ H\epsilon(z-h) \frac{2(a+z-h)^2}{[(a+z-h)^2 + x^2]^2} - \frac{1}{[(a+z-h)^2 + x^2]} \right\} + \dots \\ &= \bar{w} \frac{a}{k_o} \left\{ H\epsilon(z-h) \frac{(a+z-h)^2 - x^2}{[(a+z-h)^2 + x^2]} \right\} \quad \text{with } \mu_o = k \quad \text{and } G_o(k) = \frac{k}{k_o} + \dots \end{aligned}$$

Which is a trapped wave.

pg 490 # 3.944.12 \*\*\*\*\*

(b) - When  $la \gg 1$  (but  $k_o a < 1$ ),  $I_1 \gg I_{o_1} + I_{o_2}$ , and the wave is hydrostatic

The third integral does not contribute, because the exponential decay of the Fourier transform of the bell....

$$\begin{aligned} w(x, z) &\approx \bar{w} \int_0^\infty dk G_1(k) w_{\mu_1}(k, z) a \exp(-ak) = I_1 \\ I_1 &= \bar{w} a H\epsilon(z-h) \int_0^\infty dk \sin(\lambda(z-h) + kx) \exp(-ak) + \dots \\ &= \bar{w} \frac{a}{[a^2 + x^2]} H\epsilon(z-h) [a \sin(\lambda(z-h)) + x \cos(\lambda(z-h))] + \dots \\ &\quad \text{with } \mu_1 = l; \quad G_1(k) = 1 \quad \text{and } \lambda = \sqrt{l^2 - k_o^2} \end{aligned}$$

(c) - When  $la = O(1)$ ,  $I_{o1} \ll I_1 + I_{o2}$ , and the wave is non-hydrostatic

$$w(x, z) \approx I_1 + I_{o2} = \bar{w} \left\{ \int_0^l dk G_1(k) w_{\mu_1}(k, z) a \exp(-ka) + \int_l^\infty dk G_o(k) w_{\mu_o}(k, z) a \exp(-ka) \right\}$$

\*\*\*\*\*

---


$$I_1 = \bar{w} \int_0^l dk G_1(k) w_{\mu_1}(k, z) a \exp(-ka) \approx \bar{w} a \exp(-la) \int_0^l dk G_1(k) w_{\mu_1}(k, z)$$

$$\bar{w} a \exp(-la) H\epsilon(z-h) \left[ \sin(l(z-h)) \int_0^l dk \frac{\cos(k(x-z+h))}{\sqrt{l^2-k^2}} \right. \\ \left. + \cos(l(z-h)) \int_0^l dk \frac{\sin(k(x-z+h))}{\sqrt{l^2-k^2}} \right] + \dots$$

$$= \bar{w} la \exp(-la) H\epsilon(z-h) \frac{\pi}{2} \left[ \sin(l(z-h)) J_o(l(x-z+h)) + \cos(l(z-h)) H_o(l(x-z+h)) \right] + \dots$$

$$\text{with } \mu_1 = l - k \text{ and } G_1(k) = \frac{l}{\sqrt{l^2 - k^2}};$$

\*\*\*\*\*

---


$$I_{o2} = \bar{w} \int_l^\infty dk G_o(k) w_{\mu_o}(k, z) a \exp(-ka)$$

in the near field, large wave numbers....  $I_{o2}$  can be written in terms of incomplete  $\Gamma$  functions:

$$I_{o2} = \bar{w} la \left\{ H\epsilon(z-h) \left[ \frac{1}{2} \Gamma(0, l(a+z-h+ix)) + \frac{1}{2} \Gamma(0, l(a+z-h-ix)) \right] \right\} + \dots$$

$$\text{with } \mu_o = k; \text{ and } G_o(k) = \frac{l}{k}$$

which, through the use of the average value theorem,  $I_{o_2}$  can be written as....

$$I_{o_2} = \bar{w} a \exp(-la) H\epsilon(z-h) \int_0^\infty dk \exp(-k(a+z-h)) \cos(kx) + \dots$$

$$= \bar{w} H\epsilon(z-h) \frac{a(a+z-h)}{[(a+z-h)^2 + x^2]} + \dots \quad \text{with } \mu_o = k \quad \text{and } G_o(k) = 1$$

in the far field, wave numbers close to  $l$  .....

$$I_{o_2} = \bar{w} a \exp(-l(a+z-h)) \int_l^\infty dk \frac{\cos(kx)}{\sqrt{k^2 - l^2}} + \dots$$

$$= -\bar{w} la \frac{\pi}{2} N_o(lz) H\epsilon(z-h) \exp(-l(a+z-h)) + \dots$$

$$\mu_o = l \quad \text{and} \quad G_o(k) = \frac{l}{\sqrt{k^2 - l^2}}$$

pg 419 # 3.753.1 # 3.753.2 # 3.753.3 # 3.753.4

pg 477 # 3.893.2 \*\*\*\*\*

(d) - When  $la \ll 1$  (but  $\exp(-k_o a) \approx 1$ ),  $I_{o_2} \gg I_{o_1} + I_1$ , and the flow is irrotational

We assume  $l = 0.0$ , then....

$$w(x,z) = I_1 + I_{o_2} = \bar{w} \int_0^{k_o} dk G_1(k) w_{\mu_1}(k,z) a \exp(-ak) + \bar{w} \int_{k_o}^\infty dk G_o(k) w_{\mu_o}(k,z) a \exp(-ak)$$

Most of the contribution of  $I_1$  comes for  $k \approx k_o$ , but this contribution is canceled by very rapid oscillations,  $I_1 \approx 0.0$ .

The far field the contribution of the trapped wave  $I_{o_2}$  comes for  $k \approx k_o$ , but this contribution is canceled by very strong trapping. Therefore.....

$$I_{o_2} = \bar{w} \int_{k_1 > k_o}^\infty dk G_o(k) w_{\mu_o}(k,z) a \exp(-ak)$$

$$= \frac{u^* a}{U h} \left\{ H\epsilon(z-h) \left[ \frac{1}{2} \Gamma(0, (a+z-h+ix)k_1) + \frac{1}{2} \Gamma(0, (a+z-h-ix)k_1) \right] + \dots \right.$$

with  $\mu_o = k$ ;  $\bar{w}G_o(k) = \frac{u^{*2}}{U} \frac{1}{kh}$  and  $k_1 = \sqrt{(2)}k_o$

pg 489 # 3.941.4 \*\*\*\*\*

The  $\Gamma$ s are incomplete  $\Gamma$  functions. However, through the use of the average value theorem and since the vertical scale of the perturbation equals the depth of stress layer and because the near field the contribution of the trapped wave comes for  $k \gg k_o$ , then .....

$$I_{o2} = \frac{u^{*2}}{U} a He(z-h) \int_0^\infty dk \cos(kx) \exp(-(a+z-h)k) + \dots$$

$$= \frac{u^{*2}}{U} He(z-h) \frac{a(a+z-h)}{[(a+z-h)^2 + x^2]} + \dots \text{ with } \mu_o = k \text{ and } \bar{w}G_o(k) = \frac{u^{*2}}{U}$$

pg 477 # 3.893.2 \*\*\*\*\*

**Step function stress**

(a) Wave in a stratified atmosphere,  $I_{o1} \ll I_1 + I_{o2}$

$$w(x, z) \approx I_1 + I_{o2} = \frac{2\bar{w}}{\pi} \left\{ \int_0^l dk F_1'(k) G_1(k) \int_l^\infty dk F_o'(k) G_o(k) \right\}$$

$$I_1 = \frac{\bar{w}}{2} \frac{2}{\pi} He(z-h) \left[ \sin(l(z-h)) \int_0^l dk \frac{\sin(k(x-z+h))}{\sqrt{l^2 - k^2}} \right.$$

$$\left. - \cos(l(z-h)) \int_0^l dk \frac{\cos(k(x-z+h))}{\sqrt{l^2 - k^2}} \right] + \dots$$

$$I_1 = \frac{\bar{w}}{2} He(z-h) [\sin(l(z-h)) H_o(l(x+a-z+h)) - \cos(l(z-h)) J_o(l(x+a-z+h))] + \dots$$

$$\mu_1 = l - k \text{ and } \frac{G_1(k)}{k} = \frac{1}{\sqrt{l^2 - k^2}}$$

in the near field, large wave numbers...  $I_{o2}$  can be written in terms of  $\Gamma$  functions....

$$I_{o2} = \frac{\bar{w}}{\pi} \left\{ He(z-h) \left[ \frac{i}{2} l((z-h) + i(x+h)) \Gamma(-1, l((z-h) + i(x+h))) \right. \right.$$

$$-\frac{i}{2}l[(z-h) - i(x+h)]\Gamma(-1, l((z-h) + i(x+h))) \Big] + \dots$$

$$I_{o_2} = \frac{\bar{w}}{\pi} He(z-h)$$

$$\left\{ \left[ \frac{i}{2}l((z-h) + i(x+h))\Gamma(-1, l((z-h) + i(x+h))) \right] - \frac{i}{2}l[(z-h) - i(x+h)]\Gamma(-1, l((z-h) + i(x+h))) \right] \Big\} + \dots$$

$$\text{with } \mu_o = k; \text{ and } G_o(k) = \frac{l}{k}$$

pg 489 # 3.941.2 \*\*\*\*\*

which can be approximate to.....

$$I_{o_2} = \frac{\bar{w}}{\pi} He(z-h) \tan^{-1} \frac{x+a}{z-h} + \dots$$

$$\mu_o = k \text{ and } G_o(k) = 1$$

pg 489 # 3.941.1 \*\*\*\*\*

in the far field, wave numbers close to  $l$  .....

$$I_{o_2} = \frac{\bar{w}}{2} \frac{2}{\pi} He(z-h) \int_l^\infty dk \exp(-k(z-h)) \frac{\sin(k(x+a))}{\sqrt{k^2 - l^2}} + \dots$$

$$= \frac{\bar{w}}{2} \text{sign}(x+a) J_o(l(x+a)) He(z-h) \exp(l(z-h)) \dots$$

$$\text{and } \mu_o = l \text{ and } \frac{G_o(k)}{k} = \frac{l}{\sqrt{k^2 - l^2}}$$

pg 419 # 3.753.1 # 3.753.2 # 3.753.3 # 3.753.4

(b) Trapped wave in a non-stratified atmosphere,  $I_{o_2} \gg I_{o_1} + I_1$

$$\begin{aligned}
 w(x, z) &\approx I_{o_2} = \frac{2\bar{w}}{\pi} \int_0^\infty dk F'_o(k) G_o(k) \\
 &= \frac{u^{*2}}{2U} \frac{2}{\pi} He(z-h) \int_0^\infty dk \frac{\sin(k(x+a))}{k} \exp(-k(z-h)) + \dots \\
 &= \frac{u^{*2}}{\pi U} He(z-h) \tan^{-1} \frac{x+a}{z-h} + \dots \\
 &\text{with } \mu_o = k \text{ and } \bar{w}G_o(k) = \frac{u^{*2}}{U}
 \end{aligned}$$

pg 489 # 3.941.1 \*\*\*\*\*

### Waves in a two layers atmosphere

(a) Wave in the free atmosphere, generated in a non-stratified stress layer

Matching of the solution emerging from the stress layer into the free atmosphere we have a transmitted mode and a trapped mode:

$$w(x, z) \approx I_1 + I_{o_2}$$

$$I_1 = \frac{u^{*2}}{\pi U} He(z-h) \int_0^l dk \frac{\sin(ka)}{k} \cos(\mu_1(z-h) + kx) [1 - \exp(-2hk)] + \dots$$

and.....

$$I_{o_2} = \frac{u^{*2}}{\pi U} He(z-h) \int_l^\infty dk \frac{\sin(ka)}{k} \cos(kx) \exp(\mu_o(z-h)) [1 - \exp(-2hk)] + \dots$$

I expand the exponential in the reflected mode (emerging from the stress layer) .....

$$[1 - \exp(-2hk)] = [1 - 1 + 2hk - 2(hk)^2 + \dots] = 2hk [1 - hk + \dots]$$

furthermore.....we have:

$$\frac{\sin(ka)}{k} \cos(\mu_1(z-h) + kx) = \frac{\sin(k(a+x-z+h) + l(z-h)) - \sin(k(a-x+z-h) - l(z-h))}{2k}$$

and.....

$$\frac{\sin(ka)}{k} \cos(kx) = \frac{1}{2k} [\sin(k(a+x)) - \sin(k(a-x))]$$

in the two above eq.s the second term is the downstream mode, which we neglect.. then the trasmitted mode at the upstream transition is:

$$I_1 = \frac{u^{*2}}{\pi U} h H e(z-h) \int_0^l dk (1-hk) \sin(k(a+x-z+h) + l(z-h)) + \dots$$

then the trapped mode at the upstream transition is:

$$I_{o2} = \frac{u^{*2}}{\pi U} h H e(z-h) \int_0^\infty dk (1-hk) \sin(k(a+x)) \exp(k(z-h)) + \dots$$

and.....

$$I_1 + I_{o2} = \frac{u^{*2}}{\pi U} H e(z-h)$$

$$\left\{ h \frac{h[\sin(l(x+a)) - \sin(l(z-h))] - (x+a-z+h)[(1+hl)\cos(l(x+a)) - \cos(l(z-h))]}{(x+a-z+h)^2} \right. \\ \left. + h(x+a) \frac{(x+a)^2 + (z-h)^2 - 2h(z-h)}{[(x+a)^2 + (z-h)^2]^2} \right\}$$

pg 427 # 389 Stand. Math. Tables \*\*\*\*\*

pg 477 # 3.893.1 \*\*\*\*\*

pg 490 # 3.944.11 \*\*\*\*\*

(b) Wave ducted within the surface layer

1<sup>st</sup> - The trapped mode in the stress layer is trapped in the free atmosphere as well.

3<sup>rd</sup> - The modes ducted within the stress layer are shifted by 2h at each reflection: the mode reflected by the ground is shifted by 2h at each reflection, the mode returning from the top of the stress layer is shifted by 2h at each reflection.....

$$[H e(z) - H e(z-h)] \Gamma_{down}^m = \frac{\bar{u}}{2} \frac{2}{\pi} [H e(z) - H e(z-h)]$$



$$\begin{aligned}
& \left[ \sin(l((2m+1)h-z)) \int_0^l dk \frac{\sin(k(x - ((2m+1)h-z)))}{\sqrt{l^2 - k^2}} \right. \\
& \left. - \cos(l((2m+1)h-z)) \int_0^l dk \frac{\cos(k(x - ((2m+1)h-z)))}{\sqrt{l^2 - k^2}} \right] \\
& [He(z) - He(z-h)] \Gamma_{ref}^m = -\frac{\bar{w}}{2} \frac{2}{\pi} [He(z) - He(z-h)] \\
& \left[ \sin(l((2m+1)h+z)) \int_0^l dk \frac{\sin(k(x - ((2m+1)h+z)))}{\sqrt{l^2 - k^2}} \right. \\
& \left. - \cos(l((2m+1)h+z)) \int_0^l dk \frac{\cos(k(x - ((2m+1)h+z)))}{\sqrt{l^2 - k^2}} \right] \\
& m = 0, 1, 2, 3 \dots \quad \mu_1 = l - k \quad \text{and} \quad \frac{G_1(k)}{k} = \frac{1}{\sqrt{l^2 - k^2}}
\end{aligned}$$

2<sup>nd</sup> - The propagating mode in the stress layer (3<sup>rd</sup>), computed at z=h, is matched with trapped in the free atmosphere:

Matching of the modes emerging from the stress layer with the trapped mode in the free atmosphere:

$$He(z-h)[\Gamma_{down}^m(z=h) + \Gamma_{ref}^m(z=h)] \exp(-l(z-h))$$

$$m = 0, 1, 2, 3 \dots \quad \mu_0 = l$$